RADIO REFLECTION AND REFRACTION PHENOMENA IN THE HIGH SOLAR CORONA

RONALD N. BRACEWELL* AND GEORGE W. PRESTON
Berkeley Astronomical Department, University of California
Received July 11, 1955; revised August 19, 1955

ABSTRACT

At the lowest frequencies used in radio astronomy, e.g., at 18 Mc/s, the sun has not yet been observed; but if existing data are correct, it presents a number of curious features: (*a*) the size of the sun as a radio-frequency source is two to three times the size of the visible sun, but in place of a sharp limb, there is merely a gradual fading-away into the background; (*b*) a zone of sky is occulted by the sun, and, because significant effects of refraction reach farther out into the corona than the effects of absorption, the occulted zone is some nine times larger than the photosphere; (*c*) the sun exhibits an occulting disk whose diameter is six times that of the photosphere and which differs from the emitting disk in having a sharp limb; (*d*) the discrepancy in size between the occulted zone and the occulting disk is associated with apparent displacement of the unocculted sky toward the sun by refration; (*e*) within the occulting disk the sun behaves as a convex reflector, mirroring the whole of the unocculted sky. The reflection of the Galaxy, though greatly diminished in size, remains comparable as a radio source with the emitting sun itself. If observed with existing aerials, which are incapable of resolving the solar emission from the galactic reflection, the sun should apparently exhibit a marked annual variation of flux density.

I. INTRODUCTION

The phenomena accompanying the transfer of radio-frequency radiation in the high solar corona can best be displayed by considering the lowest radio frequencies, and in this paper attention is concentrated on a frequency of 18 Mc/s, which occupies a place of special importance in radio astronomy as representing the long-wave-length end of the atmospheric window. It is true that Jansky's original discovery of the radio emission of the Galaxy was made at a slightly lower frequency and that Higgins and Shain (1954) have succeeded in obtaining observations at 9 Mc/s, but the work which has recently proved most fruitful and offers promise of continuing to do so is that of Shain (1951, 1954), Shain and Higgins (1954), and Shain and Mitra (1954) on 18 Mc/s. For this reason we have adopted 18 Mc/s as a representative low frequency where necessary to carry our ideas to numerical conclusions.

Observation shows that at 18 Mc/s the Galaxy is the most conspicuous feature in the sky as studied with the low resolution afforded by a 17° beam. Thus at the galactic center the very high brightness temperature of 375000° K was measured by Shain. No correction was included for the smoothing effect of the aerial, and there is reason to believe that the true brightness temperature is even higher.

The poor resolving power hitherto obtainable at 18 Mc/s has allowed only a blurred view of the sky; Shain's array of 30 dipoles, which has a beamwidth of 17°, extends over half an acre. On account of its small angular size, the quiet sun does not make much contribution to a radiometer with such a wide beam, and it has therefore not yet been studied. Higher resolution is already needed to investigate an expected narrow absorption lane (due to interstellar gas) in the galactic emission. In the present paper it is shown that the sun, too, will prove of great interest.

Section II gives the primary calculations of ray paths and absorption integrals in the sun's atmosphere, using methods exemplified in work on higher frequencies by Burkhardt and Schlüter (1949), Denisse (1950), Jaeger and Westfold (1950), Smerd (1950), and Hagen (1951). Since this section augments the published calculations of ray paths and center-limb brightness distributions, by carrying them to lower frequencies, it is

* On leave from Radiophysics Laboratory, Commonwealth Scientific and Industrial Research Organization, Sydney, Australia.

presented in a form which permits its use as reference material. Published ray paths have, however, proved to be insufficiently detailed for some purposes, making it desirable that the calculations themselves should be brought within easier reach. Some attention is paid to this aspect here, it is believed, for the first time.

In Section III the primary results are used to demonstrate the existence of an occulting disk and to derive its size. For the sky outside the occulting disk the amount of refraction is given, and for the interior zone the reflection coefficient, magnification, and deviation due to the solar mirror are given.

In Section IV these results are applied in calculating the image of the Galaxy in the sun at different times of the year, with a view to exhibiting the various forms which the image can assume. The emission of the sun plus galactic image, which gives the sun's apparent flux density as measured with a radiometer incapable of resolving the two, is shown to depend on the season.

II. PRIMARY CALCULATIONS

For the purposes of the present calculations the corona is sufficiently specified by a statement of the electron density, N, and the kinetic temperature of the electrons, T_e, at all points. From these two quantities the two necessary subsidiary quantities—refractive index, n, and absorption coefficient, κ—can be deduced. The temperature will be taken as 10^6 degrees K, and the electron density will be assumed to depend on ρ, the distance from the sun's center in units of the photospheric radius, as follows:

$$N = 1.55 \times 10^{14} \rho^{-6} (1 + 1.93 \rho^{-10}) \text{ electrons/m}^3 .$$

This formula, which is based on photometry of the white light of the corona, is due to Baumbach (1937), save that a term has been omitted which represented zodiacal light (Allen 1947). In adopting this formula, we assume spherical symmetry, the consequences of which are discussed in Section V. An advantage of the formula is that numerical results become directly comparable with those of the many other authors who have used it. The refractive index n in a medium containing N free electrons/m^3, each making ν collisions/sec, is given by

$$n^2 = 1 - \frac{N e^2}{\epsilon_0 m (\omega^2 + \nu^2)} ,$$

as long as the right-hand side is not negative. This provision is fulfilled in the present work. The remaining symbols have their usual meanings (e and m, charge and mass of electron; ω, angular frequency of wave; ϵ_0, permittivity of free space $= 8.854 \times 10^{-12}$ F/m). In terms of ρ and taking $\nu \ll \omega$,

$$n^2 = 1 - 12400 f^{-2} \rho^{-6} (1 + 1.93 \rho^{-10}) ,$$

where f is in megacycles per second. When $\rho \gg 1$, we have the simpler form

$$n^2 = 1 - 12400 f^{-2} \rho^{-6} ,$$

and when $f = 18 \times 10^6$,

$$n^2 = 1 - 38.27 \rho^{-6} .$$

The correction factor $1 + 1.93\rho^{-10}$ depends on ρ as shown in the accompanying tabulation.

	ρ							
	1	1 1	1.2	1 3	1.4	1 5	1.6	1 7
$1+1\ 93\rho^{-10}$	2 93	1.74	1 31	1 14	1 07	1 03	1 02	1 01

At 18 Mc/s the refractive index falls to zero at $\rho = 1.84$ (see Fig. 1). All ray paths thus lie well out in the corona. From the refractive index variation with height, the path of a radio-frequency ray may be calculated by using Snell's laws, which take the form: (*a*) all rays lie in planes containing the center of the sun, and (*b*) for all points of a ray,

$$n\rho \sin i = a \ , \tag{1}$$

where a is a constant for that ray and i is the angle of incidence of the ray on the surface of constant refractive index (Emden 1907).

For any ray, such as that in Figure 2,

$$\frac{\rho\, d\theta}{d\rho} = -\tan i .$$

Therefore,

$$\frac{d\theta}{d\rho} = -\rho^{-1} \sin i\,(1 - \sin^2 i)^{-1/2} = -\rho^{-1}\left(\frac{a}{n\rho}\right)\left[1-\left(\frac{a}{n\rho}\right)^2\right]^{-1/2}$$

$$= \frac{-a}{\rho\,(n^2\rho^2 - a^2)^{1/2}} ,$$

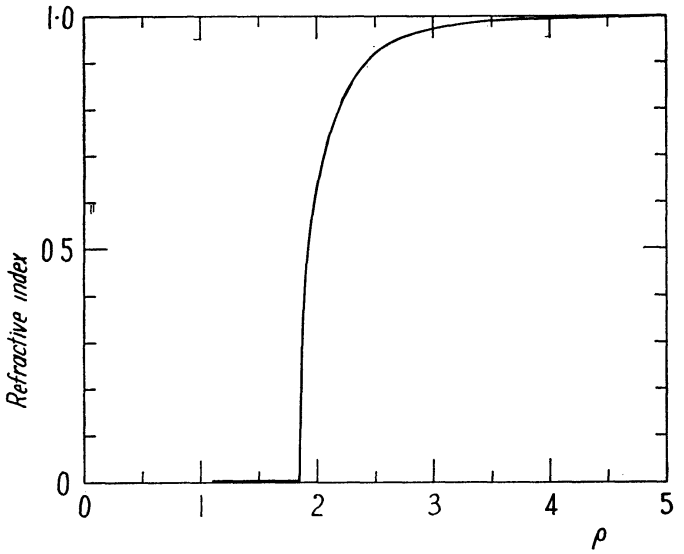

FIG. 1.—Refractive index of the corona at 18 Mc/s

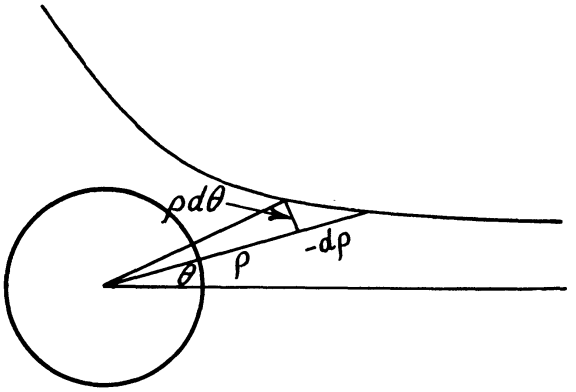

FIG. 2.—A radio-frequency ray path in the corona

and the equation of a ray is

$$\theta = a \int_{\rho}^{\infty} \frac{d\rho}{\rho\,(n^2\rho^2 - a^2)^{1/2}}. \tag{2}$$

The meaning of the constant a may be seen by going to large ρ, where $n \doteqdot 1$. Then $\rho \sin i = a$ = distance of the asymptote of the ray from the parallel line through the sun's center. This is shown on Figure 3, which also introduces ρ_a and θ_a, the polar coordinates of the turning point of a ray, and the deviation of a ray, Δ. We need the important relation,

$$n_a \rho_a = a\ , \tag{3}$$

and we may also note that

$$\Delta = \pi - 2\,\theta_a\ . \tag{4}$$

Throughout this work a and ρ will be reckoned in units of the phospheric radius.

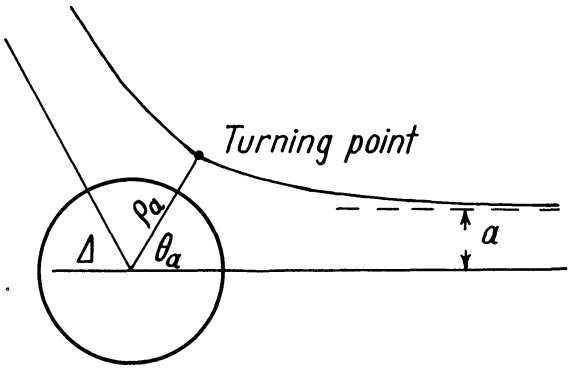

FIG. 3.—The parameters of a ray path

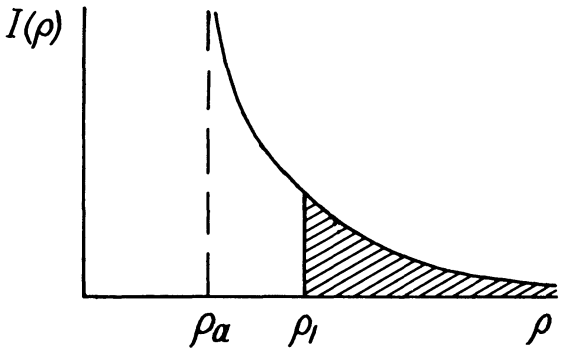

FIG. 4 —The integrand of equation (2)

Ray paths must be calculated by numerical integration of equation (2) with successively different values of a. The nature of the integrand $I(\rho) = a\rho^{-1}(n^2\rho^2 - a^2)^{-1/2}$ for a particular ray is as shown in Figure 4. The value of θ where $\rho = \rho_1$ is given by the shaded area, and the value of θ_a is the whole area under the curve.

For some purposes, a knowledge of the turning point and asymptotes of each ray might be sufficient. Given a, one can calculate ρ_a from equation (3) simply from a knowledge of the refractive index variation, and the result of this calculation is shown in Figure 5; but to get θ_a requires the integration of equation (2). Thus

$$\theta_a = a \int_{\rho_a}^{\infty} \frac{d\rho}{\rho\,(n^2\rho^2 - a^2)^{1/2}}. \tag{5}$$

The integration may be reduced to a summation as follows. Calculate $I(\rho)$ for $\rho = \rho_a + h$, $\rho_a + 2h$, $\rho_a + 3h$, . . . , as far as ρ_m, where h is a small interval and ρ_m is a large value of ρ. The sum

$$h \sum_{\rho_a+h}^{\rho_m} I(\rho)$$

will approach the required integral indefinitely as $h \to 0$ and $\rho_m \to \infty$. But in practice it is desirable for the interval h to be as coarse, and for ρ_m to be as small, as is compatible with accuracy. This leaves two end corrections. The area under the tail may be seen from physical reasoning to be arcsin $[a/(\rho_m + \frac{1}{2}h)]$, and the area of the strip in which the

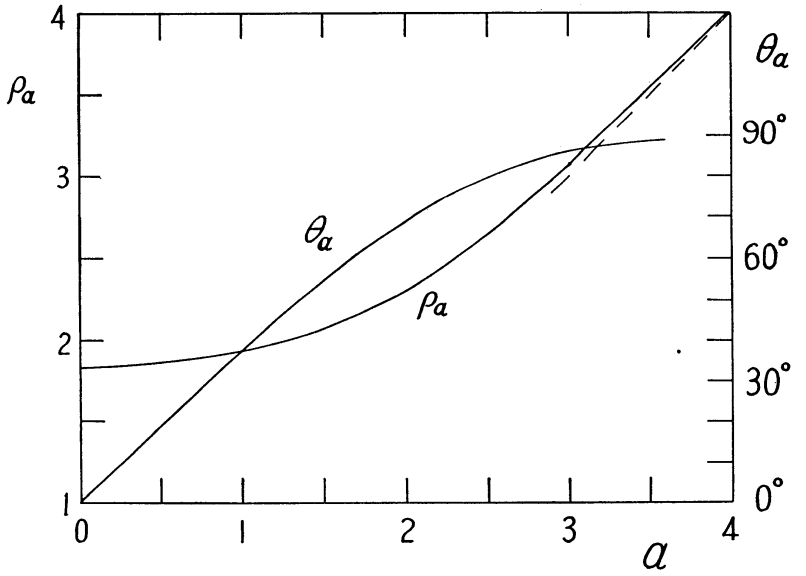

FIG. 5 —Co-ordinates of the turning points of rays

integrand goes infinite may be evaluated by a method given by Jeffreys and Jeffreys (1946). Then we have the following closed formula in place of the integral (5):

$$\theta_a = h\,[3.77I(\rho_a+h) - 0.96I(\rho_a+2h) + 1.12I(\rho_a+3h)] + h\sum_{\rho_a+4h}^{\rho_m} I(\rho) + \arcsin\frac{a}{\rho_m+\frac{1}{2}h}. \tag{6}$$

In almost every case it has been found sufficient to take $h = 0.1$ and to extend the summation, Σ, over only six terms. The values of θ_a so obtained are given, with ρ_a, in Figure 5. The ray paths themselves are shown in Figure 6.

If κ is the absorption coefficient of the corona, the optical length of a ray will be given by

$$\tau = \int \kappa\, ds\,, \tag{7}$$

where the integral is taken along the whole ray. The element of path ds can be expressed in terms of the photospheric radius $R_\odot$ as

$$ds = R_\odot\left[1 + \left(\rho\frac{d\theta}{d\rho}\right)^2\right]^{1/2} d\rho\,. \tag{8}$$

The absorption coefficient of an ionized medium depends on the collision frequency, ν, and the electron density, N, as follows:

$$\kappa = \frac{2\sqrt{2}\pi f}{c}\left\{\left[\frac{(1-x)^2+z^2}{1+z^2}\right]^{1/2} - \frac{(1+z^2-x)}{1+z^2}\right\}^{1/2}, \tag{9}$$

where x and z are the dimensionless magneto-ionic parameters,

$$x = \frac{Ne^2}{m\epsilon_0\omega^2}, \qquad z = \frac{\nu}{\omega}.$$

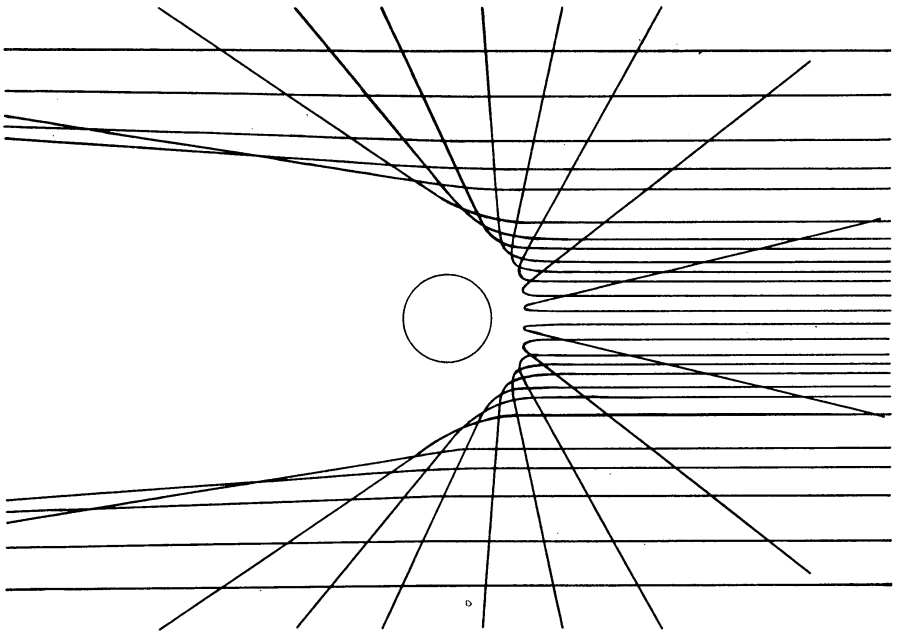

FIG 6 —Ray paths in the corona at 18 Mc/s

In place of this cumbersome expression, one can use the approximation

$$\kappa \doteq \frac{\nu x}{n c}, \tag{10}$$

provided that the refractive index n is not near zero. As n approaches zero, the absorption coefficient rises to a finite value, given approximately by

$$\kappa_{n=0} = \frac{2\sqrt{2}\pi f z^{1/2}}{c},$$

which is obtainable from equation (9) by putting $x = 1$ and $z \ll 1$. The approximate expression (10), however, becomes infinite. A corresponding approximation under which we took $n^2 = 1 - x(1+z^2)^{-1}$ in Section I is not subject to this difficulty. The full expression is

$$n^2 = \frac{1}{2}\left\{\left[\frac{(1-x)^2+z^2}{1+z^2}\right]^{1/2} + \frac{1+z^2-x}{1+z^2}\right\}^{1/2}.$$

Since it is proposed to consider the optical length of rays which pass close to the level of zero refractive index, it is necessary to examine the validity of expression (10) in the course of the numerical work. This is done below. Meanwhile, adopting the approxima-

tion, and using Smerd and Westfold's (1949) formula for the collision frequency in ionized hydrogen, we have

$$\kappa = \frac{10^{-11} N^2}{n f^2 T_e^{3/2}},$$

where T_e is the electron temperature of the medium. Taking the electron temperature of the corona to be constant over the region where absorption is important, we obtain

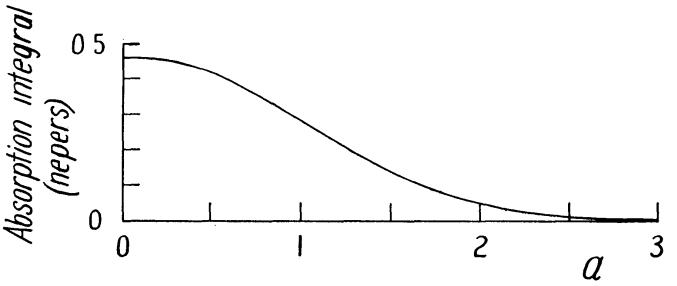

FIG. 7.—Absorption integral

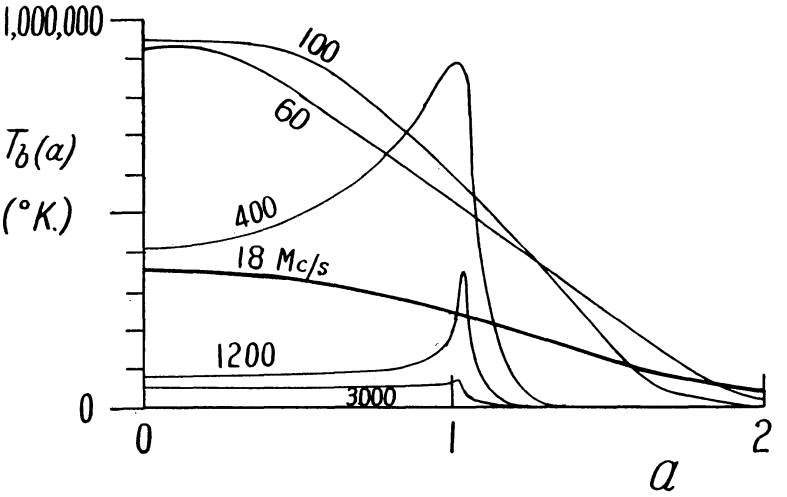

FIG 8 —Solar brightness temperature distribution over the disk at 18 Mc/s (*heavy line*) compared with that calculated for other frequencies.

the following basic equation for calculating the optical thickness of the corona taken along a ray path:

$$\tau = \frac{2 \times 10^{-11} R_\odot}{f^2 T_e^{3/2}} \int_{\rho_a}^{\infty} \frac{N^2 \rho \, d\rho}{(n^2 \rho^2 - a^2)^{1/2}}. \tag{11}$$

The absorption integrals may be performed in the same way as the ray-path integrals since the integrand becomes infinite at $\rho = \rho_a$ and tapers away to zero as ρ approaches infinity, just as in Figure 4. The result is shown in Figure 7. It may be seen that the corona is optically thin for all 18-Mc/s rays, the absorption integral being always less than half a neper.

The validity of equation (10) must now be discussed. Assuming that $T_e = 10^6$ degrees K and $f = 18$ Mc/s, the value of the absorption coefficient when $x = 1$ comes to 10^{-4} nepers/m. The approximate formula gives an infinite result for $x = 1$, but for

$x = 1$–10^{-14} this drops to 10^{-4}. The inaccurate range of the approximate formula is thus confined to levels infinitesimally close to the level where $x = 1$; and in the course of the calculations leading to Figure 7 it was confirmed that the approximation does not lead to error even for extremely small values of a.

As calculations of the kind described here have been carried out for shorter wave lengths, it is of interest to make a comparison. In Figure 8 we see solar brightness distributions calculated for the same solar model by Smerd. The lowest frequency considered was 60 Mc/s. The present result for brightness temperature $T_b(a)$, calculated from the formula

$$T_b(a) = T_e(1 - e^{-\tau}),$$

is shown as a heavy line. On 18 Mc/s the extension of the sun is seen to be greater than on higher frequencies, which continues the trend already shown and is due to the level of origin rising with decreasing frequency. On the other hand, the earlier calculations

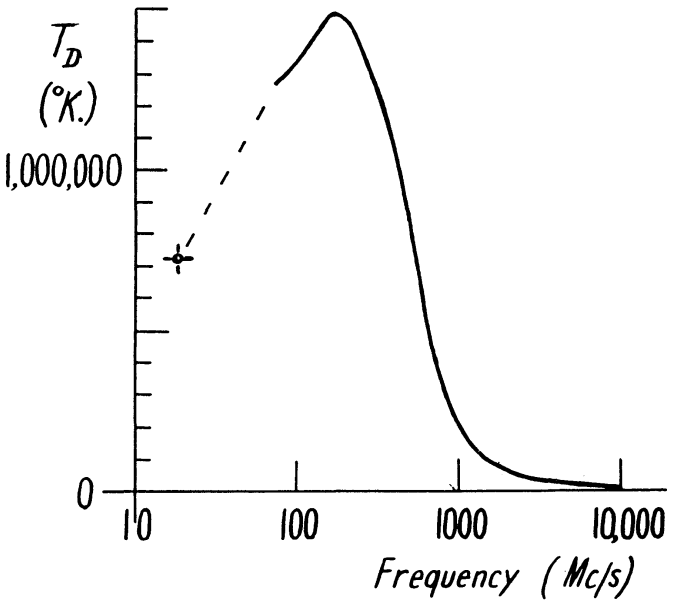

FIG. 9.—Sun's apparent disk temperature

showed, as far as they went, that the central brightness temperature of the sun increased steadily from 10^4 up to 10^6 degrees K, with decreasing frequency. However, this trend must reverse at about 60 Mc/s, since at 18 Mc/s the central brightness temperature is only 375000° K. The decreasing of the brightness temperature is due to the thinning-out of electrons as the level of origin rises with decreasing frequency.

The apparent disk temperature, T_D, which is a measure of the sun's flux density and therefore suitable for comparison with observation, is given by

$$T_D = 2\int_0^\infty T_b(a)\, a\, da\,.$$

The value obtained is 720000, and Figure 9 shows how this fits in with the results at other frequencies. The curve is the theoretical one calculated by Smerd and is well supported by observation (Pawsey and Smerd 1953). The point calculated for 18 Mc/s shows that, in spite of the greater extension of the emitting sun, the total radiation at 18 Mc/s would be expected to be well below the maximum. This has not yet been verified by observation.

III. GEOMETRICAL OPTICAL PHENOMENA

The envelope to the rays shown in Figure 6 may be termed the "limit-of-escape surface" for radiation reaching an observer at infinity on the right-hand side, since radiation originating within this enveloping surface will not be able to escape in the direction of the observer. The occulted volume cannot usefully be described in terms of an occulting disk, since the size of the disk depends on the distance of the source. If, however, we consider a family of rays which, instead of converging at infinity, converge at a finite distance, e.g., at the earth's distance from the sun, then a useful concept may be isolated. Although the appearance of Figure 6 would hardly be altered, the enveloping surface would become asymptotic to a cone having its vertex at the earth. Then, although the size of the occulting disk would increase with distance as before, its angular size would approach a constant value for sources not in the immediate vicinity of the sun. Several studies (Machin and Smith 1952; Hewish 1955) of occultation of the discrete radio source in Taurus have been made experimentally on meter wave lengths, but the only published theoretical work is that of Link (1952).

To obtain an equation for the angular size of the occulting disk, consider a family of rays passing through the earth and making angles α with the sun-earth line (Fig. 10). Let each ray make an angle β with the sun-earth line, well away from the sun on the side remote from the earth. Taking the rays in order of increasing α, we see that their inter-

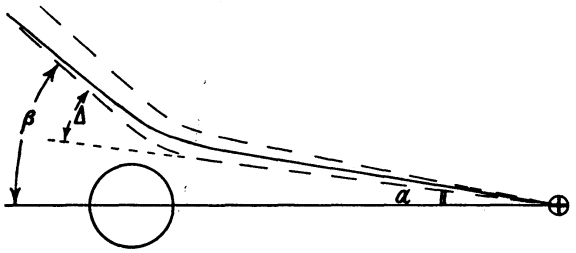

FIG. 10 —Derivation of the angular size of the occulting disk

sections with the celestial sphere have a stationary position. The locus of such points, taken in all position angles, is the rim of the occulted zone of the celestial sphere, and its position is given by

$$\frac{d\beta}{da} = 0 .$$

Since $\beta = \alpha + \Delta$ and $\alpha \doteqdot a\Omega$, where $\Omega = 0.0046$ = angular radius of photosphere, we have, in terms of quantities available from Section II,

$$\frac{d\Delta}{da} = -\Omega ,$$

or, from equation (4),

$$\frac{d\theta_a}{da} = \tfrac{1}{2}\Omega . \tag{12}$$

Reference to Figure 5 reveals that $d\theta_a/da$ does not fall to the required low value of 0.0023 in the range of a shown. We can extend the data on θ_a to larger values of a without resorting to numerical integration by utilizing the fact that for large ρ_a the ray path is not very curved. If we integrate $d\theta/d\rho$ along the straight line tangential to the ray at its turning point, we have, instead of equation (5),

$$\theta_a \doteqdot a \int_{\rho_a}^{\infty} \frac{d\rho}{\rho\,(\rho^2 - a^2)^{1/2}} = \arcsin n_a . \tag{13}$$

The approximate expression arcsin n_a will be found to give the great bulk of the accurate value in equation (5). If we now subtract equation (13) from equation (5), we have, without approximation,

$$\theta_a = \arcsin n_a + a\int_{\rho_a}^{\infty}\left[\frac{1}{\rho\,(n^2\rho^2 - a^2)^{1/2}} - \frac{1}{\rho\,(\rho^2 - a^2)^{1/2}}\right]d\rho\,.$$

The integral on the right-hand side is small and, if evaluated approximately, leads to

$$\theta_a \doteqdot \arcsin n_a + \frac{\pi}{2\sqrt{2}}(1 - n_a)^{1/2}\,.$$

From the assumed data on refractive index variation we have $1 - n_a \doteqdot 19a^{-6}$; hence

$$\theta_a \doteqdot \frac{\pi}{2} - 1.3a^{-3}\,;$$

and from equation (12) we find that, for the occulting ray,

$$a \doteqdot 6.4\,.$$

The occulting disk therefore subtends an angle of 3°.2 at the earth, and, since the deviation of the occulting ray is 0°.6, the zone of sky occulted has a diameter of 4°.4.

To an observer on the earth, a distant source in the occulted zone would not be visible. A source just outside this zone would appear to be shifted toward the sun by an amount Δ, which could be as high as 0°.6. Accompanying this shift there would be a lateral compression $\sin\alpha/\sin\beta$ and a radial expansion $d\alpha/d\beta$, with a resultant average magnification,

$$\left(\frac{\sin\alpha}{\sin\beta}\frac{d\alpha}{d\beta}\right)^{1/2}.$$

The flux density of a small discrete source would be increased by this factor.

Inside the occulting disk the terrestrial observer would see a reflection of the whole of the unocculted sky. The distortion and magnification would continue to be represented by the foregoing expression, but the magnification would now be much less than unity. The average magnification is the square root of the ratio of the solid angle subtended by the occulting disk to 4π, since almost the whole of the sky will appear reflected within the disk. This is very small, in the present case 0.014. The magnification at the center of the disk is 0.0035. This is deduced from the value of $d\theta_a/da$ at $a = 0$ (0.66), obtainable from Figure 5. As well as suffering diminution in angular size, the reflected image of a source is subject to attenuation by the amounts given in Figure 7.

To summarize this section we may say that the sun at 18 Mc/s acts as a diffuse radiating disk with a central temperature of 375000° K, about 1° in diameter. It occults a zone of sky 4°.4 in diameter and magnifies and distorts discrete sources just outside the occulted zone. Each point of the unocculted sky is seen in two places, once via the direct ray and once via the reflected ray. The situation is closely analogous to a mirage, in which an inverted image is seen by reflected rays. Though it is not often stressed in connection with the mirage, there must also be an occulted zone hidden behind the area occupied by the image.

IV. THE IMAGE OF THE GALAXY

Radio-frequency radiation from the Galaxy, reflected in the solar corona, will have a brightness temperature virtually the same as the brightness temperature of the direct radiation from the Galaxy. It is true that there will be a reduction due to absorption in the corona, and Figure 7 may be used to calculate the reduction, but for most rays it is small. In the direction of the galactic center the brightness temperature of the direct

radiation is known from the work of Shain and Higgins (1954) to be 300000° K at least. It may well be more, since the value stated is an average over a zone 17° in diameter. Now the sun itself, at the center of the disk where it is brightest, has a brightness temperature of 375000° K, as calculated previously, so it follows that the reflected image of the Galaxy is about as bright as the sun itself. Observational studies of the sun at 18 Mc/s will therefore be complicated by the reflected galactic radiation, and it is of interest to consider what the principal effects will be.

The observations of the galactic radiation are fragmentary but adequate for the present purpose, since they show the general shape of the contours of equal brightness temperature in the vicinity of the brightest part. Table 1 gives the galactic and equatorial co-ordinates of points on three representative lines of equal brightness temperature surrounding the galactic center ($l = 330°$; $b = 0$). A comparison of Table 1 with

TABLE 1

300,000 K.	l(deg.)	330	320	330	340
	b(deg.)	2.5	0	−2.5	0
	R.A.	17^h30^m	17^h15^m	17^h50^m	18^h05^m
	δ(deg.)	−23	−35	−27 5	−17 5
200,000 K	l	330	270	330	30
	b	15	0	−15	0
	R.A.	16^h48^m	12^h40^m	18^h43^m	19^h43^m
	δ	−18	−62	−33	27
150,000 K	l	330	240	330	60
	b	22.5	0	−22.5	0
	R.A.	16^h23^m	9^h20^m	19^h18^m	21^h20^m
	δ	−13	−50	−36	50

the published observations will show that the departures from symmetry about the galactic center have not been preserved. It would have been possible to do so, but the nature of the principal phenomena is better displayed by retaining only the best-established attributes of the radiation.

When the observer looks at an angular distance a (see Fig. 10) from the center of the sun's disk in position angle P measured eastward from the south point of the disk, his line of sight passes through the point on the celestial sphere which is in the same position angle but at an angular distance β from the center of the disk. Let T_G be the galactic brightness temperature at that point, τ the optical length of the ray, and T_S the contribution of solar emission to the brightness temperature. Then the observed brightness temperature T in the direction (a, P) will be given by

$$T(a, P) = T_G(\beta, P)\, e^{-\tau} + T_S(a).$$

Since for small values of a there is no distinction between a and a, we may replace $T_S(a)$ by $T_b(a)$, as given in Figure 8, and take τ directly from Figure 7. To calculate $T_G(\beta, P)$, one might first use Figure 5 and the relation $\beta = a + \pi = 2\theta_a$ to obtain β from a, and then convert the co-ordinates (β, P) to galactic co-ordinates (l, b), taking account of the co-ordinates of the sun, and interpolate in Table 1 to find T_G. It is in this last step that practical difficulties arise, but a very neat procedure has been found which is based on the preliminary construction of two charts, Figures 11 and 12.

Figure 11 represents the relation

$$T = T_G e^{-\tau} + T_S$$

in terms of a and T_G as independent variables, the data on τ and T_S being incorporated.

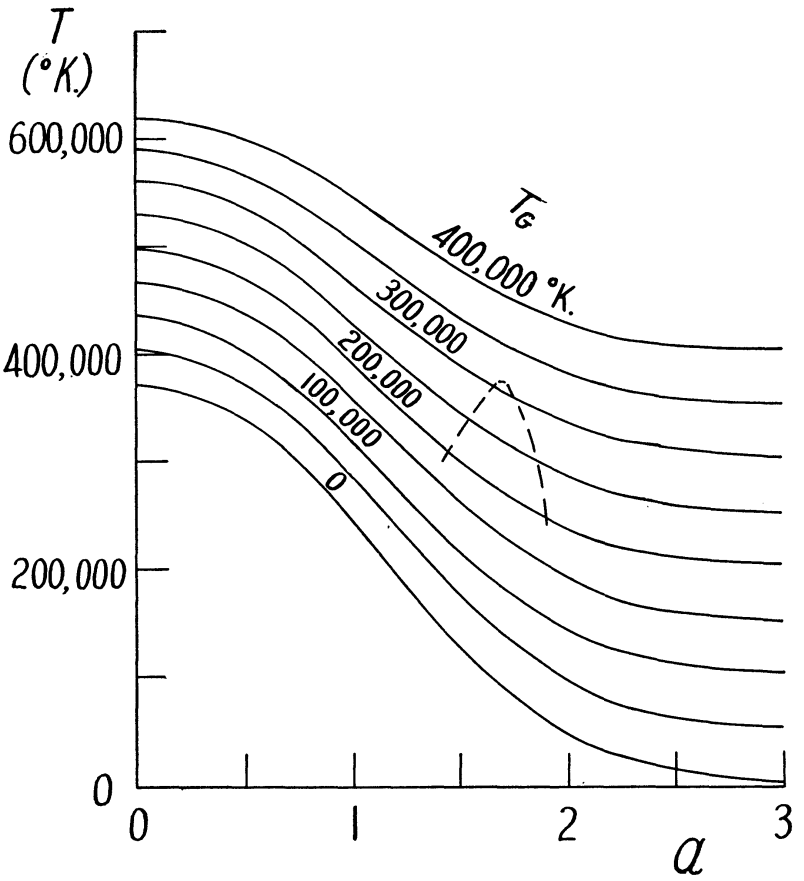

FIG. 11.—The brightness temperature, T, of a ray a which emerges from the Galaxy with brightness temperature, T_G.

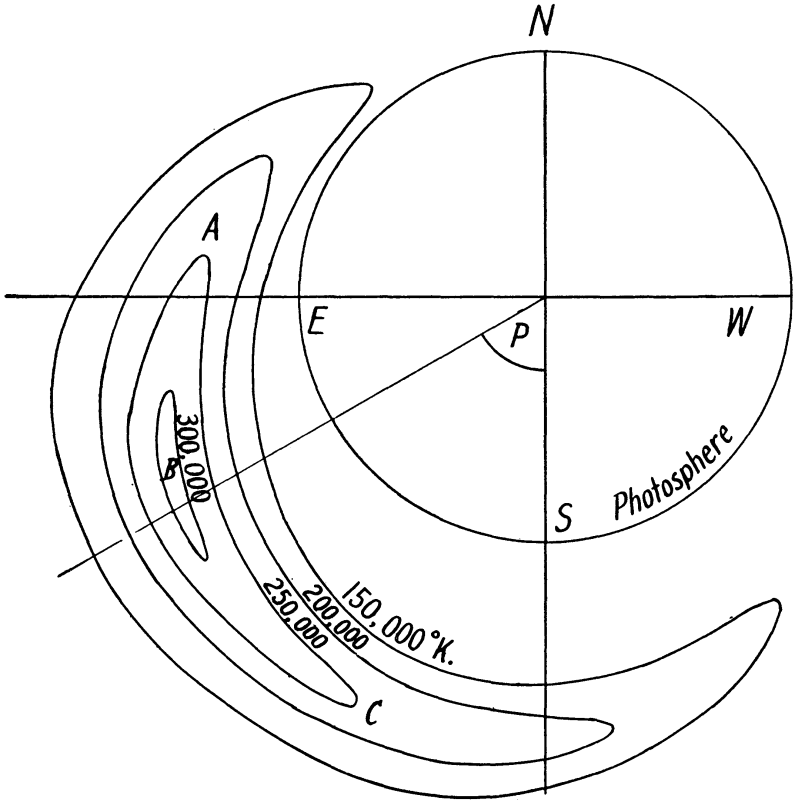

FIG. 12.—The image of the Galaxy before allowing for solar emission and absorption (October 21)

Figure 12 shows the image of the Galaxy, as calculated before allowance for solar emission and absorption. The co-ordinates of the solar center were fixed as for October 21, and then the pair of values of right ascension and declination from Table 1 were converted to α and P by the relations

$$\cos \alpha = \sin \text{dec.} \sin \text{dec.}_\odot + \cos \text{dec.} \cos \text{dec.}_\odot \cos (\text{R.A.} - \text{R.A.}_\odot) ,$$

$$\cot P = \tan \text{dec.} \cos \text{dec.}_\odot \operatorname{cosec} (\text{R.A.} - \text{R.A.}_\odot) - \sin \text{dec.}_\odot \cot (\text{R.A.} - \text{R.A.}_\odot) ,$$

the latter of which is conveniently reduced to addition and subtraction by the use of Norie's nautical tables.

Now consider a cross-section of the image along any line such as that shown in position angle P and plot it on Figure 11 to the curvilinear co-ordinates T_G and a. The broken line, which shows the result, is then a cross-section of the desired distribution, and it enables one to mark the points where any contour T = Const. crosses the section line.

In this way one rapidly builds up the contour diagram of brightness temperature over the sun and vicinity (Fig. 13). The distribution obtained shows a region exceeding 350000° K at the center of the disk and a further region which, from its brightness and extent, is clearly comparable in flux density with the sun alone. The contour on which the brightness is half the central value (*shown broken*) is roughly circular, but distinctly eccentric, though not in the direction of the galactic center.

Observation of the sun with limited resolving power should therefore reveal the following effects: (*a*) flux density increased, (*b*) position shifted, and (*c*) symmetry, if observable, impaired. All these effects depend on the season and, to some extent, on the resolution of the aerial. The dependence on season may be exhibited roughly by showing the distance of the galactic image from the sun's center and its orientation, as in Figure 14. For the purposes of this figure a segment of the galactic equator, 120° long, is shown in its reflected position. No allowance is made for solar emission and absorption; thus for October 21 the arc shown is the same as *ABC* in Figure 12. It is probably correct to deduce from Figure 14 that the flux density of sun plus image goes through a deep minimum in June, since in that month the image is smallest and subject to the greatest attenuation.

It is possible that solar flux density measurements already in progress on higher frequencies contain a small contribution from the Galaxy, but the extent to which the reflection effects persist at higher frequencies remains to be studied.

V. DISCUSSION

Several assumptions have been made in the foregoing analyses, and we here consider to what extent they could modify the conclusion that the sun should present an appearance like that shown in Figure 13. The main assumptions are (*a*) the corona is isothermal at 10^6 degrees K; (*b*) the electron density is given by the Baumbach-Allen formula as far out as six solar radii; and (*c*) the corona is spherically symmetrical.

The assumed temperature of the corona affects the solar emission and the attenuation of the galactic radiation in such a way that if the corona were hotter, the solar emission would be less and the galactic reflection brighter, thus emphasizing the image phenomenon. The evidence that the corona is kept fairly isothermal by its high thermal conductivity and that it is at a temperature which cannot be below about a million degrees is based on independent radio and optical observations, and there is now little question that this broad fact is established. Should the temperature fall off at the large distances here discussed, the solar emission would be unaffected, and the increased absorption of the image would, because of the small electron density, be negligible.

As regards the electron-density distribution, there is no sound basis for extrapolating the distribution established for the inner corona to a value of $\rho = 6$. There is evidence,

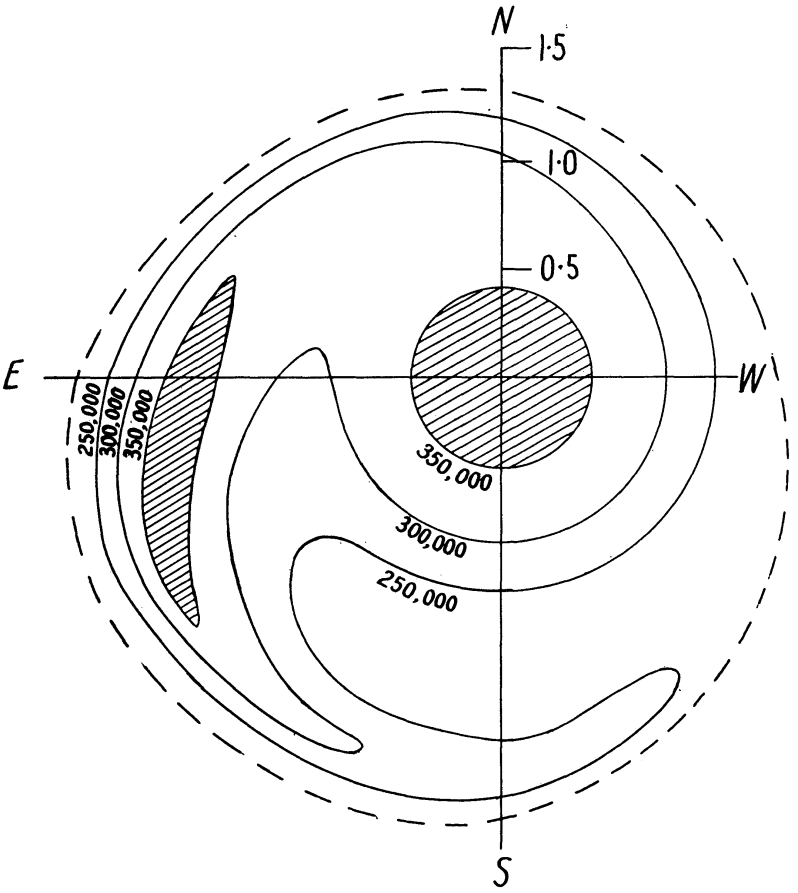

FIG. 13.—Solar brightness distribution showing the reflection of the Galaxy Brightness temperatures in degrees Kelvin. The approximate half-central-brightness contour is shown in broken outline.

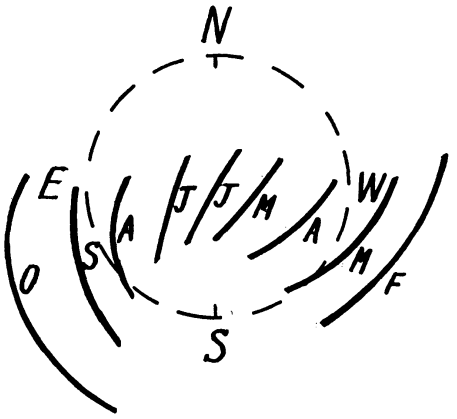

FIG. 14.—The position of the galactic image in different months of the year. The photosphere is shown in broken outline.

however, that at these greater distances the electron density is larger than the value given by the formula (Machin and Smith 1952). The result of such a modification to the present theory would be to enlarge the occulting disk and the angular dimensions of the image of the Galaxy. Therefore, as far as the temperature and electron-density data are concerned, the phenomena described here are likely to be, if anything, more pronounced than we have calculated.

Departures of the corona from symmetry may introduce major modifications to the present results. For example, a coronal streamer in which the electron density was ten times greater than the surrounding value could displace the level of zero refractive index by a substantial fraction of a solar radius. This seems to be the most probable major cause of discrepancy between theory and future observation and, under adequate resolution, could permit electron-density studies in the outer parts of the coronal streamers. The necessary modifications to the theory, in the sector affected, should not be much more arduous than at present, since in any case we are forced to use numerical methods; so it is probable that gross departures of the observations from the simple theory could be interpreted. In considering this subject, the analogy with the mirage is useful for suggesting the types of distortion to be expected. The phenomena of towers, duplicated images both erect and inverted, indentations, and detached occulating patches are all to be expected under various kinds of variation of refractive index.

A different type of departure from symmetry has been invoked by Hewish (1955) to explain the occultation observations on the discrete source in Taurus. He finds radio evidence for a cloudy structure of the corona probably associated with the fine visible structure. The effect on a point source of radio waves is to spread it out over a disk a few minutes of arc in diameter; but unless the instrument used had extremely high resolution, as did his interferometer, this effect would not be distinguishable from the inherent blurring due to the instrument. To what extent regular refraction was affected is not clear, but one can imagine that, in the case of extreme non-uniformity of ionization, regular refraction phenomena could be obliterated. The solar reflector would become a diffuse reflector. It does not seem worth while at present to consider this theoretically, since the likelihood on present evidence is that reflection will be partly diffuse over the whole sun and possibly very diffuse in places.

It would seem that the major features of the visible white-light corona would be the major causes of asymmetry of the 18-Mc/s reflector. However, it may be remembered that, on account of the rapid decrease of electron density with ρ, the contours of equal electron density are not distorted very much from the spherical form by coronal features which are visually quite marked.

The general conclusion from this discussion of assumptions is that we are likely to have covered the principal effects on 18 Mc/s. These are in themselves so interesting that forthcoming observations with high resolution on 18 Mc/s will be awaited with impatience, and it may be expected that in due course such observations will lead to definite knowledge about the electron density and its degree of uniformity in the outer solar corona, under both quiet and disturbed conditions.

REFERENCES

Allen, C. W. 1947, *M.N.*, **107**, 426.
Baumbach, S. 1937, *A.N.*, **263**, 121.
Burkhardt, G., and Schlüter, A. 1949, *Zs. f. Ap* , **26**, 295.
Denisse, J.-F. 1950, *Ann. d'ap.*, **13**, 181.
Emden, R. 1907, *Gaskugeln* (Leipzig: B. G. Teubner Verlag), p. 296.
Hagen, J. P. 1951, *Ap. J.*, **113**, 547.
Hewish, A. G. 1955, *Proc. R. Soc. London, A*, **228**, 238.
Higgins, C. S., and Shain, C. A. 1954, *Australian J. Phys.*, **7**, 460.
Jaeger, J. C , and Westfold, K. C. 1950, *Australian J. Sci. Res. A*, **3**, 376.

Jeffreys, H., and Jeffreys, B. S. 1946, *Methods of Mathematical Physics* (Cambridge: At the University Press), p 264
Link, F. 1952, *Bull. Centr Astr. Inst. Czechoslovakia*, **3**, 6.
Machin, K. R., and Smith, F. G 1952, *Nature*, **170**, 319.
Pawsey, J L , and Smerd, S F 1953, *The Sun*, ed. G P. Kuiper (Chicago: University of Chicago Press), chap. 7.
Shain, C A. 1951, *Australian J. Sci. Res A*, **4**, 258
——— 1954, *Australian J. Phys* , **7**, 150
Shain, C. A , and Higgins, C S. 1954, *Australian J. Phys.*, **7**, 130.
Shain, C. A., and Mitra, A P 1954, *J. Atm and Terr. Phys* , **5**, 316.
Smerd, S. F 1950, *Australian J Sci. Res. A*, **3**, 34.
Smerd, S. F , and Westfold, K C 1949, *Phil Mag* , **40**, 831.